The Formation and Growth of Protein Precipitates in a Continuous Stirred-Tank Reactor

C. E. Glatz
Department of Chemical Engineering
Engineering Research Institute
Iowa State University
Ames, IA 50011

Michael Hoare, Jaime Landa-Vertiz
Department of Chemical and
Biochemical Engineering
University College London,
Torrington Place
London WC1, England

Product particle size distribution data are obtained for the isoelectric precipitation of protein in a continuous stirred reactor in order to evaluate the kinetics of aggregate growth in processes for protein recovery via precipitation. Data are modeled using population balances to verify the postulated mechanism and provide a basis for evaluating results for other reactor configurations. Aggregate breakage was found to be the dominant phenomenon.

SCOPE

Precipitation can play an important role in the downstream processing of biological products, in particular, proteins. Such a separation technique plays a dual role of product concentration and enrichment. The next step is invariably a solid-liquid separation whose efficiency is dependent on the size and stability of the precipitate.

We have measured particle size distributions for protein precipitated in a continuous stirred tank by addition of sulfuric acid to bring the extract feed to the isoelectric point. The effect of protein concentration and mean shear rate in the vessel are assessed. Analysis of the data is done in the light of a population balance model for number density vs. size. The model accounts for growth as a pseudocontinuous addition of small particles to a growing aggregate due to the spatial variation of turbulence. Aggregate breakage is described as a power law function of aggregate size. The model is derived from earlier efforts (Grabenbauer and Glatz, 1981; Petenate and Glatz, 1983b), and benefits from the wider range of data reported here as well as the large amount of data published more recently on the behavior of protein precipitates (Bell and Dunnill, 1982a; Bell et al., 1983; Hoare, 1982a; Hoare et al., 1982; Virkar et al., 1982).

The data are also presented in the alternate format of characteristic sizes of the distribution, permitting easier discussion and compilation of size data from a variety of reactor configurations. The results are of interest as a special case of aggregation phenomena, unique in that the particle sizes are small enough to be within the Kolmogorov microscale.

CONCLUSIONS AND SIGNIFICANCE

The data make clear the limitation that breakage exerts on the attainable particle size in protein precipitation. It is apparent that size can be increased if protein concentration is increased. The larger sizes are more efficient at collecting newly formed solid material; hence higher linear growth rates are obtained. The population balance model is able to fit the data quite

Correspondence concerning this paper should be addressed to Michael Hoare or C. E. Glatz.
The present address of Jaime Landa-Vertiz is Juan Racine 130-401, Chapultapec Morales, 11570, Mexico, D.F.

well using three parameters, even when one of these is restricted in a manner consistent with previous experimental results. The value of the growth parameter is consistent with theoretical collision frequencies for the postulated mechanism. Agreement with theoretically expected parameter dependencies on shear rate and concentration are qualitatively correct but fall short quantitatively. In the case of the breakage function, this shortcoming may well be the result of inadequate models for the aggregate structure. A correlation is demonstrated for size vs. mean shear rate that is applicable to batch and continuous stirred reactors and tubular continuous reactors of various sizes. Only the mean size for the tubular reactor seems to deviate. The model results support the hypotheses that breakage is by fragmentation and that collisions between larger aggregates are ineffective for growth.

Introduction

Reactor configuration

The first stage of a process for the recovery or fractionation of proteins by precipitation involves contacting a protein stream with a precipitating agent in a reactor. Various design requirements have been discussed (Bell et al., 1983; Hoare et al., 1983; Salt et al., 1982; Virkar et al., 1981). For ensuring uniform and reproducible conditions during precipitation, advantages are apparent in the use of continuous, as opposed to batch, reactors.

To date we have examined the use of continuous stirred-tank reactors (CSTR) using HCl for the isoelectric precipitation of dilute (0.1–0.3 kg/m^3) solutions of soy protein (Grabenbauer and Glatz, 1981; Petenate and Glatz, 1983a), a continuous tubular reactor (Virkar et al., 1982), and a batch stirred reactor (Bell and Dunnill, 1982a; Hoare et al., 1982); the latter two reactor types employed concentrated soy protein solution (2.5 to 80 kg/m^3) with H_2SO_4 as a precipitating agent.

In all cases basic primary particles are formed whose size is dependent on the protein concentration and the precipitant (Nelson and Glatz, 1985). These particles continue to collide because of shear-controlled collisions to form irregularly shaped aggregates, the size of which is also determined by shear-controlled breakup. In the tubular reactor the protein is rapidly (<1 s) brought to the final precipitation condition, i.e., the isoelectric point of pH 4.8. In a batch reactor the first stage of precipitation occurs in much the same manner as in the tubular reactor except that the protein is exposed to a range of pH values. Resulting differences in size (Chan et al., 1982), shape (Bell and Dunnill, 1982a), and centrifuge performance (Bell and Dunnill, 1982b) have been reported.

In a CSTR the protein is exposed almost immediately to the correct environment for precipitation. This leads to potential advantages in avoiding overprecipitation of the protein. The shear field in a CSTR may be somewhat similar to a batch reactor, but there is a wide range of precipitate residence times. As opposed to tubular or batch reactors, fresh protein precipitates in the presence of existing aggregates. These differences, along with a preference for continuous operation, have led to the examination of isoelectric soy protein precipitation in a CSTR under conditions comparable with previous batch (Bell and Dunnill, 1982a) and tubular reactor studies (Virkar et al., 1982). Also, because the CSTR operation is more amenable to theoretical modeling (Petenate and Glatz, 1983b; Grabenbauer and Glatz, 1981), its use may lead to a fundamental understanding of precipitate formation and shear breakup.

Model solution

Physical Model. The mathematical model incorporates the following physical features and simplifying assumptions:

1. Protein comes out of solution very quickly and therefore an accounting is needed only for the solid material. This is supported by tubular reactor studies (Virkar et al., 1982; Chan et al., 1985) where precipitation, in terms of removal of soluble protein, is completed within 1 s for the protein concentrations above 2 kg/m^3.
2. Growth of an aggregate occurs by collision with primary particles and smaller aggregates. However, collisions between larger aggregates are ineffective in forming lasting aggregates. Growth is therefore viewed as the incremental addition of small units to the growing aggregates.
3. The effectiveness of those collisions of small particles with growing aggregates is independent of the size of the collecting species.
4. Aggregates break up to form a small number of daughter fragments of significant mass. The number of daughter fragments would tend to be greater for larger parent aggregates, and this is approximated as an average fragment number dependent on the mean size of the distribution. Daughter fragments are assumed to be of equal volume.

Population Balance. The particle size distribution is described by a population balance on aggregates of size L which, for a CSTR at steady state, mean residence time τ, and with no particles in the feed, reduces to

$$\frac{d(Gn)}{dL} + \frac{n}{\tau} + D - B = 0 \tag{1}$$

G, D, B, and n may be functions of L.

Expressions for each of these terms have been proposed (Petenate and Glatz, 1983b) and as used here they are of the form

$$G(L) = A\phi_1 V_g L = K_o L \tag{2}$$

$$D(L) = k' V_g \left(\frac{\mu V_g}{\sigma_{ya}}\right)^{\delta} n(L) = kL^{\beta} n(L) \tag{3}$$

$$B(L) = f \cdot D(f^{1/3} L) \tag{4}$$

where A incorporates the collision effectiveness. The model parameters are K_o, k, β, and f. The death and birth expressions assume that total particle volume is conserved and that a power

law describes the increased susceptibility of aggregates to breakup as size increases. The growth term assumes that collision due to the spatial variation of turbulence is the predominant factor, as has been demonstrated (Yuu, 1984).

The resulting equation relating number density to size is

$$\frac{dn}{dL} = \frac{k}{K_o} L^{\beta-1} [f^{\beta/3+1} n(f^{1/3}L) - n] - \frac{n}{L}\left(1 + \frac{1}{\tau K_o}\right) \quad (5)$$

An alternative expression (Grabenbauer and Glatz, 1981), discussed later results from assuming that the growth rate is independent of size. The boundary condition used is that the calculated total volume of aggregates equals the measured aggregate volume.

Past work has suggested that for a given protein concentration, β and f could be fixed at reasonable values, leaving only two fully variable parameters. Once f and β were assigned, a nonlinear least-squares routine (Iowa State University Computation Center, IMSL Library ROUTINE ZXSSQ) was used to find the values of the two remaining parameters giving the best fit to the experimental data. In this procedure the original channel number densities were represented by a fifth-order Chebyshev polynomial, permitting calculation of eleven equispaced residuals in the least-squares calculation. The numerical solutions were obtained using a fourth-order Runge-Kutta method, converging on the volume boundary condition via a shooting method using trial values for the number density at the largest size (volume was negligible beyond this size).

Number of Daughter Fragments. The existing data on breakup of protein precipitates (Bell and Dunnill, 1982a) are for capillary shear. It shows that breakup of large aggregates results in two or more main fragments and a number of small fragments comprising relatively little mass. The latter can be neglected in the balance, although they will increase and be accounted for by ϕ_1 as they are considered capable of being growth units. The larger aggregates formed the greater number of daughter fragments. However, Pandya and Spielman (1982) found that allowing for this within a given distribution of kaolin-$Fe(OH)_3$ flocs was no better than using a constant $f = 2.5$.

Breakage Power. The role of β is to describe the sharpness of the size dependence of breakage frequency. Previous workers have used the same power law formulation for breakage. Reported values have ranged from 1.0 for chemical flocs (Pandya and Spielman, 1982), up to 2 for droplets (Narsimhan et al., 1980), and as high as 3.0 for an earlier model of protein precipitation (Petenate and Glatz, 1983b). Narsimhan et al. found the higher values to be associated with smaller drops (<23 μm in their work).

Materials and Methods

A soy protein total water extract (TWE) was prepared by a 30 min extraction of defatted soy flour (Soy Fluff 200 W, Oppenheimer Casing Co. [UK] Ltd., London) in pH 9 NaOH. Solutions were prepared containing 3 kg/m^3 or 25 kg/m^3 total protein (Buiret assay). The precipitating agent used was 3.4% w/w sulfuric acid.

The CSTR was designed to standard configuration: volume, 0.27 L; height = dia., 0.07 m; one six-flat-bladed disk turbine, 0.0233 m dia., mounted centrally 0.0233 m above reactor base; four baffles 0.007 m wide; and temperature control using a water-cooled jacket. Precautions taken to avoid air-liquid interfaces were as previously described (Foster et al., 1976; Hoare, 1982a). Deaeration was not required. An airtight Teflon seal was used as the stirrer shaft entry point and bearing.

Sulfuric acid was added at constant rate using a syringe pump via a capillary, 5×10^{-5}m dia., into the impeller tip. A Jabsco impeller pump was used to feed the soya protein solution. For all experiments the protein feed rate was 3.33×10^{-7} m$^3 \cdot$ s^{-1}, and the acid feed rate was 1.4×10^{-9} m$^3 \cdot$ s^{-1} for 3 kg/m^3 protein concentration and 11.2×10^{-9} m$^3 \cdot$ s^{-1} for 25 kg/m^3 protein. A Kent EIC combination electrode was used to monitor pH near the top of the reactor. By slight variation in acid flow rate, pH could be controlled to 4.8 $\pm$ 0.03 units.

Reactor operating conditions were chosen to avoid streaming and dead spots. On the basis of tracer studies (Hoare, 1982a) these were:

$$Re > 1{,}500 \quad (6)$$

$$\frac{\tau}{\theta} > 50 \quad (7)$$

where Re is the mixing Reynolds number ($=\rho N d^2/\mu$). From Novak and Rieger (1975) we have for a six-blade, disc-turbine stirred, baffled vessel:

$$\theta = \frac{50}{N} \quad (8)$$

The mean velocity gradient, V_g, in the reactor was characterized by:

$$V_g = \left(\frac{P}{V\mu}\right)^{1/2} \quad (9)$$

where P/V was obtained from a correlation (Novak and Rieger, 1975). The TWE and protein precipitate suspensions are Newtonian over the range of shear rates likely to be encountered in the reactor (Hoare et al., 1982). For 3 kg/m^3 protein, the viscosity of the TWE was 1.1×10^{-3} N $\cdot$ s $\cdot$ m^{-2} and of the precipitate suspension 1.2×10^{-3} N $\cdot$ s $\cdot$ m^{-2}; corresponding viscosities for 25 kg/m^3 protein were 1.5 and 1.6×10^{-3} N $\cdot$ s $\cdot$ m^{-2}, respectively (Virkar et al., 1982).

Precipitation was carried out for a range of stirrer speeds 185 to 1,060 rpm. At least 10 volume changes were allowed in the reactor for steady state conditions to be achieved. On exit from the reactor the precipitate was diluted, using pH 4.8, 0.07 M sodium acetate, to <0.2 kg/m^3 within 6 s to prevent any change in aggregate size (Virkar et al., 1982). A Coulter counter, model TA II, fitted with a 70 or 140 μm dia. orifice, was used for particle size analysis. Several readings were taken to ensure that steady state conditions had been achieved.

Data for 0.15 kg/m^3 protein at three agitation levels were taken from earlier work (Grabenbauer and Glatz, 1981).

Results and Discussion

Size distributions

Size distributions from representative runs over the range of stirrer speeds are shown in Figures 1a and 1b. For both concen-

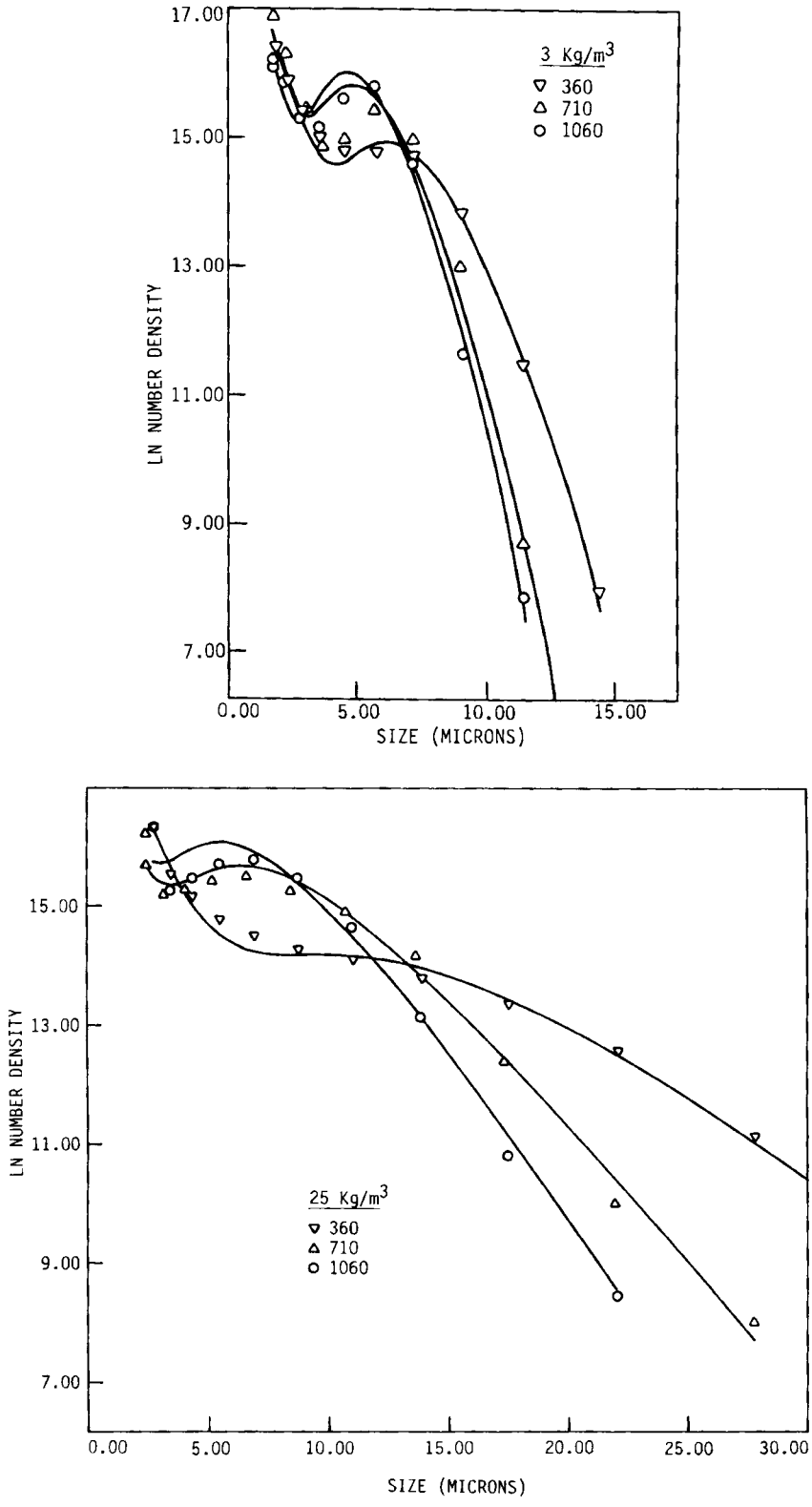

Figure 1. Particle (number) size distributions for isoelectric soya protein precipitates at three levels of stirrer speed (rpm) showing shear-limited growth.

Points: experimental data. Curves: model fits using Eq. 5.

trations studied, 3 kg/m^3 and 25 kg m^3 protein, the precipitate size decreases with increased stirrer speed, and in nearly all the cases studied there is a local maximum in the number density profile. Both of these trends are indicative of a fragmentation process during precipitate growth and breakup in the reactor (Grabenbauer and Glatz, 1981).

Preparation of precipitates under similar reactor conditions but for different protein concentrations is examined in Figure 2. Data from Grabenbauer and Glatz taken at 0.15 kg/m^3 using a different reactor, acid, and soya source are included for comparison. While there is a marked effect of protein concentration on aggregate size, the number density profiles all follow similar patterns. The trend of increasing size with higher protein concentration has also been reported for a low residence time, continuous tubular reactor (Virkar et al., 1982), and to a lesser extent for long residence time, batch reactors (Hoare et al., 1982; Bell and Dunnill, 1982a).

Modeling of number density distributions

Preliminary model studies, not shown here, indicated that the trends observed with mean velocity gradient or protein concentration in the values of growth or breakup rate constants were largely independent of the choices of β and f. Hence, to reduce the number of variable parameters while retaining reasonable agreement with the experimental number density profiles, we fixed values of $\beta = 1.5$ and $f = 3$ when modeling the preparation of the larger precipitate aggregates obtained at protein concentration of 25 kg/m^3. For the smaller precipitate aggregates prepared at lower protein concentrations, 0.15 and 3 kg/m^3, the most suitable values were $\beta = 2.3$ and $f = 2$. The trends in β and f with aggregate size agree with the experimental observations reported earlier.

Two models were examined to get the particle size data presented in Figures 1 and 2. The model based on a growth rate independent of aggregate size gave reasonable fits (results not shown here) by residual sum-of-squares criteria except at high protein concentrations. However, at all protein concentrations studied the predicted curves were biased in the manner in which they deviated from experimental observation. This was particularly evident at small sizes where the local minimum/maximum traits were largely lost. The second model examined here, Eq. 5, based on a growth rate linear in aggregate size, Eq. 2, gave satisfactory fits of the particle size data (in fact, for most runs the model fit the experimental points more closely than did the six-parameter Chebyshev polynomial on which the model fitting was actually based) and also successfully described the local minimum/maximum traits. The curves presented in Figures 1 and 2 are based on this model; it is the results obtained using Eq. 5 that are used in any further analysis.

Dependence of model parameters, k and K_o on reactor operation conditions

The theoretical description for the postulated growth mechanism shows K_o to depend on the mean velocity gradient and the volume fraction of growth units. For the protein concentrations studied, 3 kg/m^3 and 25 kg/m^3, ϕ_1 remains relatively constant. For instance, at 535 rpm, when concentration increases 8× (and ϕ, 6×), ϕ_1 (5.5×10^{-5}, estimated as the measured volume frac-

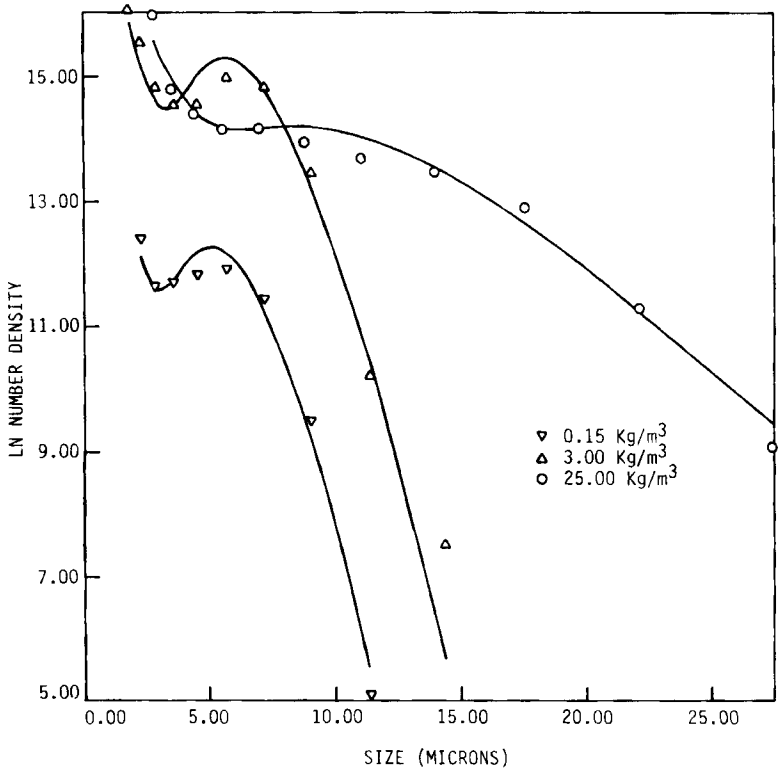

Figure 2. Particle (number) size distributions for isoelectric soya protein precipitates at three levels of total protein concentration.

Points: experimental data. Curves: model fits using Eq. 5. Data at 0.15 kg/m^{-3} from Grabenbauer and Glatz (1981). All data are for mean shear rate of approx. 200 s^{-1}.

tion solids below 2.8 μm) does not increase at all. Hence, there is little variation in K_o (6.10×10^{-4} to 6.59×10^{-4} s^{-1} in this case), with varying protein concentration, for precipitate prepared under equivalent mixing conditions. Data from the previous precipitation studies (different acid, reactor, and soy source) at 0.15 kg/m^3 protein also show a similar value for K_o even though ϕ_1 is substantially decreased (to 1×10^{-6}) in this case. However, for the latter data it was not possible to get sufficient aggregate size data at the fine end of the distribution, and it is this size that has the most significant effect on the value of K_o.

The growth rate constant also appears to be independent of stirrer speed or mean velocity gradient, a result inconsistent with the model presented in Eq. 2. ϕ_1 was found to increase slightly with V_g (5.5×10^{-5} to 6.1×10^{-5} over the range of stirrer speeds at 3 kg protein/m^3), so the product $\phi_1 V_g$ surely increases. Part of this discrepancy is undoubtedly a decrease in collision efficiency with V_g (Adler, 1981). This same insensitivity of the growth parameter to mean velocity gradient has been noted in droplet coalescence/breakup (Zeitlin and Tavalarides, 1972).

The variation of breakup rate constant with mean velocity gradient is shown in Figure 3 where, for the three protein concentrations studied, we have:

$$k\alpha V_g^{0.41} \tag{10}$$

From Eq. 4 we have:

$$kL^{\beta}\alpha \frac{V_g^{(1+\delta)}}{\sigma_{ya}^{\delta}} \tag{11}$$

Since the aggregate yield stress, σ_{ya}, decreases with increased size, L (Tambo and Hozumi, 1979), positive values of the breakage power β will result in positive values of δ. Therefore, the predicted dependence of the breakup rate constant is greater than that experimentally observed.

Several factors affecting breakup are not accounted for by the model. The same growth and breakup functions are applied to the full range of aggregate sizes. The only step function employed confines the volume fraction of growth units to particles or small aggregates. No such step function is applied to the breakup of aggregates. It might be expected that aggregates larger than the microscales of turbulence within the reactor would break up in a fashion different from those smaller than the microscales of turbulence (Tomi and Bagster, 1978). Such analysis is complicated by the range of scales of turbulence that would be experienced in a turbine-stirred reactor, but some of the aggregates formed at the highest protein concentration are likely to be susceptible to other mechanisms.

The model used also assumes a time-independent behavior of the precipitate aggregates. Within a CSTR, precipitate aggregates are exposed to a wide range of residence times and velocity gradients. Increased exposure to shear leads to precipitate aggregates more resistant to shear breakup. Bell and Dunnill (1982a) have shown that for isoelectric precipitate preparation in a batch stirred reactor, optimal aggregate strength is obtained if the product of V_g and t is such that $V_g t > 10^5$. This increase in aggregate strength largely results from a mechanism of reshaping of weak irregular aggregates prepared under low residence time shear conditions ($V_g t \sim 10^4$) into more compact aggregates. For the CSTR results presented in this paper, $V_g \tau$ ranges from 4×10^4 to 4×10^5. Allowing for the range of residence times of precipitates in the reactor, it is evident that we are dealing with a wide range of precipitate materials of differing resistances to shear breakup.

Finally, growth may also depend on aggregate history. Aging of precipitate, at the same mixing conditions as used for preparation, leads to a continual decline in size (Hoare, 1982b), suggesting that freshly prepared precipitate aggregates are more capable of further aggregation as compared to aged particles. This result was observed elsewhere for exposure of flocculated particles to shear (Smith and Kitchener, 1978).

Representative measures of precipitate size distribution

For design purposes, a more concise characterization of precipitate aggregate size is preferred to the entire population size

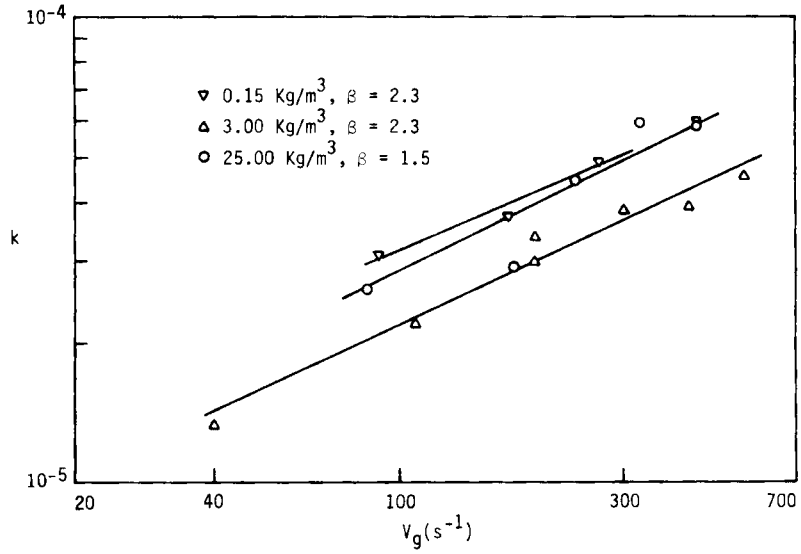

Figure 3. Breakup constant k as a power law function of mean shear rate V_g for three levels of total protein concentration.

Choices of power law exponent β (discussed in text) affect magnitude and slope, but trends are unchanged.

distribution. Two common measures are the sizes at which there are 50 or 90% by volume oversize, L_{50} and L_{90}, respectively. The latter is representative of the fine end of the size distribution and is one of the measures of the precipitate properties that is useful for centrifuge specification. The former has been correlated with membrane flux characteristics in protein precipitate recovery by crossflow membrane processes (Devereux and Hoare, 1984).

The trends in L_{50} and L_{90} with mean velocity gradient and protein concentration are described in Figure 4. Such data emphasize the dynamic interplay that exists between shear-controlled collisions leading to growth and shear-controlled breakup. Increased mean velocity gradient leads to greater relative increase in the breakup rate compared to the growth rate, giving smaller values for L_{50} and L_{90}. This is reflected in the model parameters where the shear dependence is quite evident in the breakup constant, k (Figure 3), and not detected in the growth constant, K_o. An illustration of the sufficiency of assuming K_o independent of shear rate and the power law relation of Figure 3 to describe the shear dependence of breakup is also seen in Figure 4. There the broken curves are calculated from Eq. 5 using the above two assumptions to obtain values for K_o and k.

The increase in L_{50} and L_{90} is simply a reflection of the higher number densities of colliding particles, n. Several factors explain why this is not apparent in K_o. First, the linear growth rate, G, of a given aggregate is the product of K_o and L, where the latter factor accounts for the observed faster growth at high concentration. Second, the obligatory collection of greater amounts of precipitated material at higher concentrations is accounted for by the product of G and n, both of which increase. As a result of this increased collection capacity, the increase in the volume concentration of small particles, ϕ_1, that might be expected with increase in protein concentration does not occur to any appreciable extent.

Finally, one might check to see if the model has actually accounted for growth and breakup independently or whether there will be some interaction with the power law constant, β, whose lower value at high concentrations is more tolerant of large sizes. Changing β from 2.3 to 1.5 (e.g., for the run at 3.0 kg/m^3, 710 rpm) increased K_o only 1.5%, while k increased 480% and the residual sum-of-squares increased 430%. The dominant interaction remains within the breakup function between β and k. Further support for the growth term is the agreement between calculated and experimental values. Using typical values of $V_g = 200\ s^{-1}$ and $\phi_1 = 6 \times 10^{-5}$ along with $A = 0.103$ (assuming a collision efficiency of 1, Petenate and Glatz, 1983b)

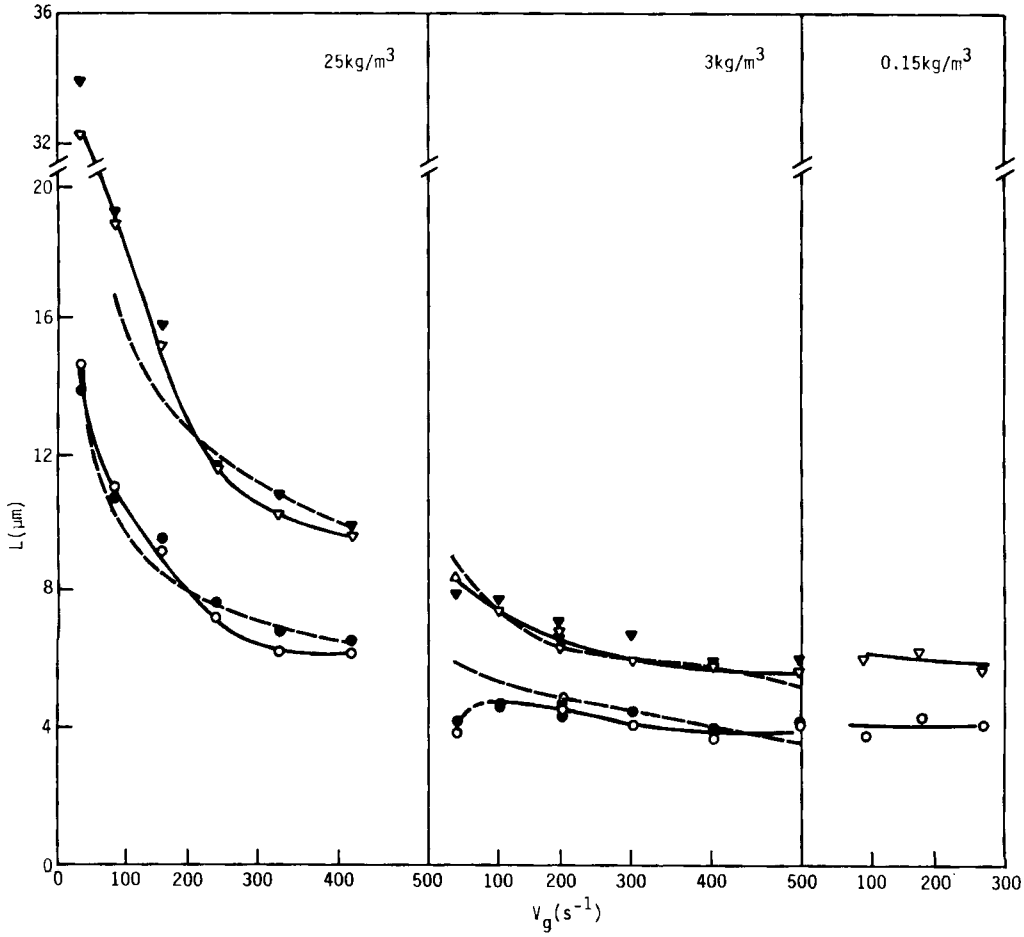

Figure 4. Size/mean shear rate dependence and size/concentration dependence for all runs.

Size distribution data from Figs. 1 and 2 are presented in two characteristic sizes, L_{50} (open and closed inverted triangles) and L_{90} (open and closed circles) (see text). Open symbols: calculated from Chebyshev polynomial fit to experimental data. Closed symbols: calculated from model fits for each run.----calculated from model using average value of K_o at each concentration and a value of k from the correlations of Fig. 3.

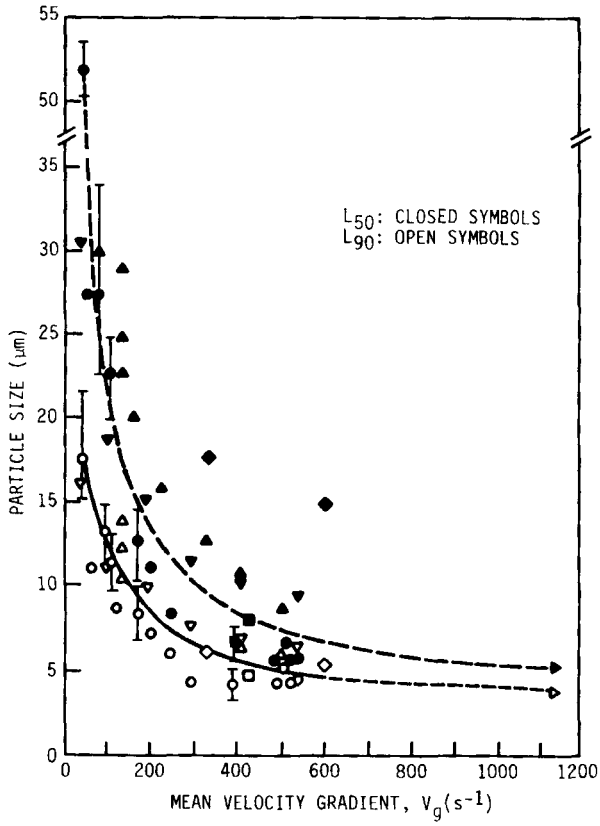

Figure 5. Relationship between reactor mean velocity gradient V_g and particle size for isoelectric soya protein precipitate.

pH 4.8; overall protein concentration 25 kg/m^{-3}; protein precipitated 85–90%.
Open symbols, L_{90}; closed symbols, L_{50}; vertical bars, range of experimental values.
Reactor type and mean residence time:
△ ▲0.27 *L* batch, 600 s (Hoare et al., 1982)
○ ● 0.67 *L* batch, 600 s (Hoare et al., 1982)
▷ ▶ 1.2 *L* batch, 600 s (Devereaux and Hoare, 1985)
□ ■ 200 *L* batch, 600 s (Bell and Dunnill, 1982b)
◇ ◆ Continuous-flow tubular, flow rate 8.3×10^{-4} to 12.5×10^{-4} m^3/s^{-1} (Virkar et al., 1982)
▽ ▼ 0.27 *L* continuous stirred tank, 811 s (this study)
Temperature, 298 K.

in Eq. 2 gives a predicted value of $K_o = 1.2 \times 10^{-3}\ s^{-1}$. Thus, a reasonable collision efficiency of one-half would bring the predicted value into agreement with observed values.

The prevailing role of shear-controlled breakup in determining final particle size is confirmed in Figure 5. For a range of reactor types and sizes it is apparent that the fine end of the distribution, L_{90}, follows the same relationship with velocity gradient. This range includes low residence time tubular reactors, batch stirred-tank reactors, and the CSTR described in this paper. However, the average size of the distribution, L_{50}, does not correlate as well with mean velocity gradient. This is partly a reflection of the variation of precipitate properties with exposure to shear. As mentioned previously, prolonged shear exposure changes surface features of the colliding species and their likelihood of forming aggregates. Precipitate prepared in a low residence time (~20 s) tubular reactor is still relatively capable of further aggregation. Also, the shear field in a tubular reactor does not include the large differences seen in the bulk and impeller regions of a stirred tank. It is likely in the case of the stirred tanks that the impeller region conditions will determine the breakup rate and hence the larger end of the size distribution.

Acknowledgment

This work was supported by grants from the National Science Foundation (CPE 8120568) and the Scientific Research Council, England.

Notation

A = collision frequency constant
B = birth rate, no./l^4t
D = death rate, no./l^4t
d = impeller diameter
f = number of equal-size daughter fragments
G = growth rate, l/t
K_o = growth constant (size-dependent growth), t^{-1}
k = breakage rate constant, $t^{-1}l^{-\beta}$
k' = proportionality constant
L = size, (l)
L_{50} = size above which is found 50% of particle volume
L_{90} = size above which is found 90% of particle volume
l = length
m = mass
N = stirrer speed, t^{-1}
n = number density, no./l^4
P = power input to stirred vessel, ml^2/t^3
t = time, (t)
V = volume, l^3
V_g = mean shear rate/velocity gradient, t^{-1}

Greek letters

β = breakage power
δ = power law constant
θ = mixing time (95% of completion), t
μ = viscosity ($m/l \cdot t$)
ρ = density, m/l^3
σ_{ya} = aggregate yield strength, m/lt^2
τ = residence time, t
ϕ = aggregate volume fraction
ϕ_1 = volume fraction of "small" particles (growth units)

Literature cited

Alder, P. M., "Heterocoagulation in Shear Flow," *J. Colloid Interface Sci.*, **83,** 106 (1981).
Bell, D. J., and P. Dunnill, "Shear Disruption of Soya Protein Precipitate Particles and the Effect of Ageing in a Stirred Tank," *Biotechnol. Bioeng.*, **24,** 1,271 (1982a).
———, "The Influence of Precipitation Reactor Configuration on the Centrifugal Recovery of Isoelectric Soya Protein Precipitate," *Biotechnol. Bioeng.*, **24,** 2,319 (1982b).
Bell, D. J., M. Hoare, and P. Dunnill, "The Formation of Protein Precipitates and their Centrifugal Recovery," *Adv. in Biochem. Eng./Biotech.*, **26,** 1 (1983).
Chan, M. Y. Y., D. J. Bell, and P. Dunnill, "The Relationship between the Zeta Potential and the Size of Soya Protein Precipitate Particles," *Biotechnol. Bioeng.*, **24,** 1,897 (1982).
Chan, M. Y. Y., M. Hoare, and P. Dunnill, "The Kinetics of Protein Precipitation by Different Reagents," accepted for publication in *Biotechnol. Bioeng.*, (1985).
Devereux, N., and M. Hoare, "Membrane Separation of Protein Precipitates: Studies with Crossflow in Hollow Fibres," *Biotechnol. Bioeng.*, accepted for publication (1984).
Foster, P. R., P. Dunnill, and M. D. Lilly, "The Kinetics of Protein Salting-out: Precipitation of Yeast Enzymes by Ammonium Sulphate," *Biotechnol. Bioeng.* **18,** 545 (1976).
Grabenbauer, G. C., and C. E. Glatz, "Protein Precipitation—Analysis of Particle Size Distribution and Kinetics," *Chem. Eng. Comm.*, **12,** 203 (1981).
Hoare, M., "Protein Precipitation and Precipitate Ageing: Salting-out and Ageing of Casein Precipitates," *Trans. Inst. Chem. Eng.*, **60,** 79 (1982a).

———, "Protein Precipitation and Precipitate Ageing: Growth of Protein Precipitates during Hindered Settling or Exposure to Shear," *Trans. Inst. Chem. Eng.*, **60,** 157 (1982b).
Hoare, M., et al., "Disruption of Protein Precipitates during Shear in Couette Flow and in Pumps," *Ind. Eng. Chem. Fundam.*, **21,** 402 (1982).
Hoare, M., D. J. Bell, and P. Dunnill, "Reactor Design for Protein Precipitation and its Effect on Centrifugal Separation," *Annals NY Acad. Sci.*, **413,** 254 (1983).
Narsimhan, G., D. Ramkrishna, and J. P. Gupta, "Homogenization Efficiency of Helical Ribbon and Anchor Agitators," *AIChE J.*, **26,** 991 (1980).
Nelson, C. D., and C. E. Glatz, "Primary Particle Formation in Protein Precipitation," *Biotechnol. Bioeng.*, **27,** 1,434 (1985).
Novak, V., and F. Rieger, "Homogenization Efficiency of Helical Ribbon and Anchor Agitators," *Chem. Eng. J.*, **9,** 63 (1975).
Pandya, J. D., and L. A. Spielman, "Floc Breakage in Agitated Suspensions: Theory and Data Processing Strategy," *J. Colloid Interface Sci.*, **90,** 517 (1982).
Petenate, A. M., and C. E. Glatz, "Isoelectric Precipitation of Soy Protein. 1: Factors Affecting Particle Size Distribution," *Biotechnol. Bioeng.*, **25,** 3,049 (1983a).
———, "Isoelectric Precipitation of Soy Protein. 2: Kinetics of Protein Aggregate Growth and Breakage," *Biotechnol. Bioeng.*, **25,** 3,059 (1983b).
Salt, D. J., et al., "Factors Influencing Protein Structure during Acid Precipitation: A Study of Soya Proteins," *Eur. J. Appl. Microbiol. Biotechnol.*, **14,** 144 (1982).
Smith, D. K. W., and J. A. Kitchener, "The Strength of Aggregates Formed in Flocculation," *Chem. Eng. Sci.*, **33,** 1,631 (1978).
Tambo, N., and H. Hozumi, "Physical Characteristics of Flocs. II: Strength of Floc," *Water Res.*, **13,** 421 (1979).
Tomi, D. T., and D. F. Bagster, "The Behavior of Aggregates in Stirred Vessels. I: Theoretical Considerations on the Effects of Agitation," *Trans. Inst. Chem. Eng.*, **56,** 1 (1978).
Virkar, P. D., et al., "Studies of the Effects of Shear on Globular Proteins," *Biotechnol. Bioeng.*, **23,** 425 (1981).
Virkar, P. D., et al., "Kinetics of Acid Precipitation of Soya Protein in a Continuous-Flow Tubular Reactor," *Biotechnol. Bioeng.*, **24,** 871 (1982).
Yuu, S., "Collision Rate of Small Particles in a Homogeneous and Isotropic Turbulence," *AIChE J.*, **30,** 802 (1984).
Zeitlin, M. A., and L. A. Tavalarides, "Fluid-Fluid Interactions and Hydrodynamics in Agitated Dispersions: A Simulation Model," *Can. J. Chem. Eng.*, **50,** 207 (1972).

Manuscript received May 1, 1985, and revision received Oct. 14, 1985.